

Available online at [www.sciencedirect.com](http://www.sciencedirect.com)**ScienceDirect**

Energy Procedia 82 (2015) 737 – 743

---

---

Energy  
**Procedia**

---

---

ATI 2015 - 70th Conference of the ATI Engineering Association

## Small size single-axis PV trackers: control strategies and system layout for energy optimization

Roberto Bruno<sup>\*</sup>, Piero Bevilacqua, Luigi Longo, Natale Arcuri*Mechanical, Energetic and Management Engineering Department – University of Calabria – Via P. Bucci 46/ C – 87036 – Arcavacata di Rende (CS) – Italy*

---

### Abstract

Solar tracking allows the increment of the electric production of photovoltaic modules; single-tracker systems can increase the collected solar radiation by 30% more than traditional fixed devices. Usually, mechanical movement systems are energy intensive and require periodic maintenance, with correspondent higher investment costs compared to traditional fixed plants. In this paper, particular single-tracking PV modules with reduced width and weight moved by low power actuators, are considered. Two different control strategies concerning the rotation angle of modules around a horizontal tilted axis, have been investigated. With reference to typical climatic data of south Italy, the problem of the modules self-shading has been analysed by evaluating the optimal layout of the whole system in order to optimize energy production.

© 2015 The Authors. Published by Elsevier Ltd. This is an open access article under the CC BY-NC-ND license (<http://creativecommons.org/licenses/by-nc-nd/4.0/>).

Peer-review under responsibility of the Scientific Committee of ATI 2015

*keywords:* PV tracking systems, control strategies, energy optimization, TRNSYS simulation, self-shading effect

---

### 1. Introduction

In the field of renewable sources, photovoltaic systems (PV) represent the most important resource for the production of non-fossil electric energy. To increase electric production, PV systems can adopt sun-tracking mechanisms: in function of the location, annual production increments ranging from 30 to 40% are reported [1]. Tracking systems can be equipped with a single or double rotation axes. The first are usually tilted and oriented toward south, by following the movement of the sun in the east-west direction.

---

<sup>\*</sup> Corresponding author. Tel.: +39 0984 494158; fax: +39 0984 494673.  
E-mail address: [roberto.bruno@unical.it](mailto:roberto.bruno@unical.it).

Dual axis trackers maintain the collection surface always perpendicular to sunlight by maximizing the incident beam solar radiation.

Several authors have investigated the performances of different tracker systems. Pavel et al. analysed experimentally and theoretically tracking bifacial PV systems [2]. Helwa et al. compared fixed and orientable PV systems to assess the auxiliary power consumptions and the effect of tracker accuracy on electric production [3]. Chicco et al. experimentally assessed the production of PV systems in orientable and fixed operations for three different locations [4]. Abu-Khader et al. carried out an experimental investigation on the effect of using multi-axes sun-tracking systems on electrical generation under Jordanian climate conditions [5]. In [6] an innovative sun-tracking system, where the movement of a photovoltaic module was controlled by using a programmable logic-controller (PLC) unit, was designed. In [7] a simpler sun-tracker that operates only at three different daily angles (1A-3P), based on the previous research by Huang and Sun [8], is proposed. In [9] the effect of using different sun-tracking mechanisms were investigated by comparing them with fixed devices, by observing that the adoption of a two-axis sun tracking system leads to a small increment of the produced electrical energy with reference to different single-axis sun tracking systems with tilted horizontal axis. Tracking systems are complex, energy intensive and expensive compared to fixed plants, since active trackers use motors and other devices to position the PV module in accordance with precise control strategies. The additional components increase investment costs especially in low power plants where the size-effect becomes crucial. Usually it is not recommended to use tracking systems for small solar panels because of the high auxiliary energy requirements: in fact the power consumption of the tracking device could be 2~3% of the increased energy [1].

In this paper the annual energy production of a small size PV system with particular geometrical characteristics which adopts a single-axis tracking system was determined. The PV system is constituted by independent strings, mounted in parallel, rotating around a horizontal tilted axis oriented toward south (see Fig. 1). The modules have reduced width and weight in order to limit the actuators' energy requirements. Two different control strategies concerning the module rotation angles, were investigated. The first is simpler since it rotates the modules in function of the solar azimuth angle; in summer, when the sun is positioned behind the collectors, this rotation angle is set to 90° compared to the horizontal plane. The second control strategy dynamically adjusts the rotation angle in order to minimize the incident angle of the beam solar radiation during the whole year. Regarding the climate data of a south Italian locality, the modules' self-shading effect was analysed by the TRNSYS code to evaluate the optimal layout of the whole system for energy optimization [11].

#### Nomenclature

$\beta_a$	inclination angle of the rotation axis (°);
$\gamma$	module azimuth (°);
$\gamma_a$	rotation axis azimuth (°);
$\gamma_s$	solar azimuth (°);
$i$	incident angle (°);
$\xi$	module inclination angle (°);
$\theta$	module rotation angle (°);
$\zeta$	solar zenith angle (°)
$D$	String spacing (m);
$F$	Fraction of shaded beam radiation (-);
$W$	string width (m);

## 2. Relationship between rotation angle and sun position

In order to evaluate the optimum rotation angle  $\theta$  of a module with a single-tracking axis oriented toward south ( $\gamma_a=0$ ), that minimizes the incident angle  $i$ , the relation between the inclination axis angle  $\beta_a$ , the panel azimuth angle  $\gamma$  and the module inclination angle  $\xi$  (evaluated between the surface normal  $n$  and the vertical direction) is required. From Fig. 1, by means similar triangles, the angle  $\xi$  results a function of the rotation angle  $\theta$  and of the tilted axis angle  $\beta_a$  given by the relation:

$$\xi = \arccos(\cos[\theta] \cdot \cos[\beta_a]) \quad (1)$$

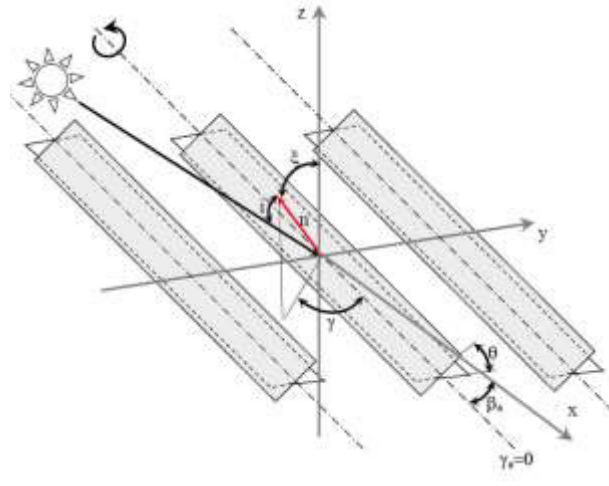


Fig. 1 – Fundamental angles describing panel and sun position

The panel azimuth  $\gamma$ , in function of a generic angle  $\gamma_a$  and for  $\beta_a \neq 0$ , can be evaluated by Eq. (2). The latter relation is valid also for  $\theta$  angles falling outside the range  $-90^\circ \sim +90^\circ$ , condition that occurs when the solar azimuth ( $\gamma_s$ ) is  $90^\circ$  greater than the axis azimuth:

$$\begin{aligned} \gamma &= \gamma_a - \arcsin\left(\frac{\sin[\theta]}{\sin[\xi]}\right) - 180^\circ \\ &\text{if } -180^\circ \leq \theta \leq -90^\circ \\ \gamma &= \gamma_a - \arcsin\left(\frac{\sin[\theta]}{\sin[\xi]}\right) + 180^\circ \\ &\text{if } +90^\circ \leq \theta \leq +180^\circ \end{aligned} \quad (2)$$

The incident angle  $i$  in function of the zenith angle  $\zeta$ , can be evaluated by [12]:

$$\cos[i] = \cos[\gamma_s - \gamma] \cdot \sin[\zeta] \cdot \sin[\xi] + \cos[\zeta] \cdot \cos[\xi] \quad (3)$$

and by introducing the angles determined from Eq. (1) and (2) in Eq. (3), the following relation can be obtained with simpler trigonometric identity for a south facing tracking axis ( $\gamma_a=0$ ):

$$\cos[i] = \cos[\theta] \cdot \{ \cos[\gamma_s] \cdot \sin[\zeta] \cdot \sin[\beta_a] + \cos[\zeta] \cdot \cos[\beta_a] \} + \sin[\theta] \cdot \sin[\zeta] \cdot \sin[\gamma_s] \quad (4)$$

In order to identify the rotation angle  $\theta$  that minimizes the incident angle  $i$ , Eq. (4) was minimized:

$$\frac{d \cos[i]}{d\theta} = -\sin[\theta] \cdot \{ \cos[\gamma_s] \cdot \sin[\zeta] \cdot \sin[\beta_a] + \cos[\zeta] \cdot \cos[\beta_a] \} + \cos[\theta] \cdot \sin[\zeta] \cdot \sin[\gamma_s] = 0 \quad (5)$$

from which:

$$\theta = \arctan\left\{ \frac{\sin[\zeta] \cdot \sin[\gamma_s]}{\cos[\gamma_s] \cdot \sin[\zeta] \cdot \sin[\beta_a] + \cos[\zeta] \cdot \cos[\beta_a]} \right\} + K \quad (6)$$

$K$  is null if the fraction of Eq. (6) is zero, or if the fraction and the panel azimuth angle are both null, or if they are both negative. If the same fraction provides a positive result but the panel azimuth is negative,  $K$  must be set to  $-180^\circ$ , contrarily if the fraction is negative but the panel azimuth is positive,  $K$  is  $+180^\circ$

[13]. By means of Eq. (6), a parametric study in function of the axis inclination angle  $\beta_a$  was conducted in order to maximize the beam solar radiation incident at a yearly level. In Tab. 1, the direct normal radiation and the solar beam radiation, in function of the axis inclination angle, are reported for the city of Cosenza (Lat.  $39.3^\circ$  N) at a monthly and annual level, for both the considered module rotation strategies. The value  $\beta_a=30^\circ$  provides the best results if the result of Eq. (6) is adopted. By comparing the two control strategies at an annual level,  $\beta_a=30^\circ$  with an optimized rotation angle increases the beam radiation by 5.8% compared to the first control strategy, and the beam collected solar energy is 27.5% greater at an annual level than a fixed module surface tilted by  $30^\circ$ , with a maximum deviation of 34.8% in June and a minimal deviation of 16.1% in January.

Table 1 – Cosenza: direct normal radiation (DNI) and beam solar radiation ( $\text{kWh/m}^2$ ) collected on the panel surface in function of the axis inclination angle, with the considered control strategies for the module rotation

	DNI ( $\text{kWh/m}^2$ )	Optimized rotation angle								In function of the solar azimuth							
		10°	20°	30°	40°	50°	60°	70°	80°	10°	20°	30°	40°	50°	60°	70°	80°
Jan	94	67	75	82	88	92	93	92	89	65	75	82	88	91	93	92	89
Feb	122	98	107	114	119	121	121	118	113	97	107	114	119	121	121	118	113
Mar	179	162	170	176	178	177	173	165	155	161	169	174	177	176	171	164	154
Apr	190	184	189	190	187	182	173	162	149	177	181	182	180	175	169	159	148
May	227	225	226	223	216	206	193	178	163	201	202	200	196	190	182	172	160
Jun	271	269	268	263	253	240	224	206	188	229	229	226	221	214	205	195	183
Jul	278	276	276	271	262	250	234	216	198	241	241	239	234	227	217	206	193
Aug	260	256	259	258	253	243	230	215	197	240	242	242	239	232	222	210	196
Sep	203	190	198	202	203	200	193	183	171	188	195	199	199	197	191	182	171
Oct	139	117	126	133	137	139	138	133	127	117	126	133	137	138	137	133	127
Nov	119	88	98	106	113	117	118	117	113	87	97	106	113	117	118	117	113
Dec	112	77	87	96	104	109	111	111	109	75	86	96	103	109	111	111	109
Yearly	2194	2007	2079	2115	2114	2075	2001	1898	1771	1877	1949	1993	2005	1987	1938	1860	1755

In Fig. 2, a comparison between the rotation angles obtained with the considered control strategies for a winter (a) and a summer day (b) is reported for  $\beta_a=30^\circ$ .

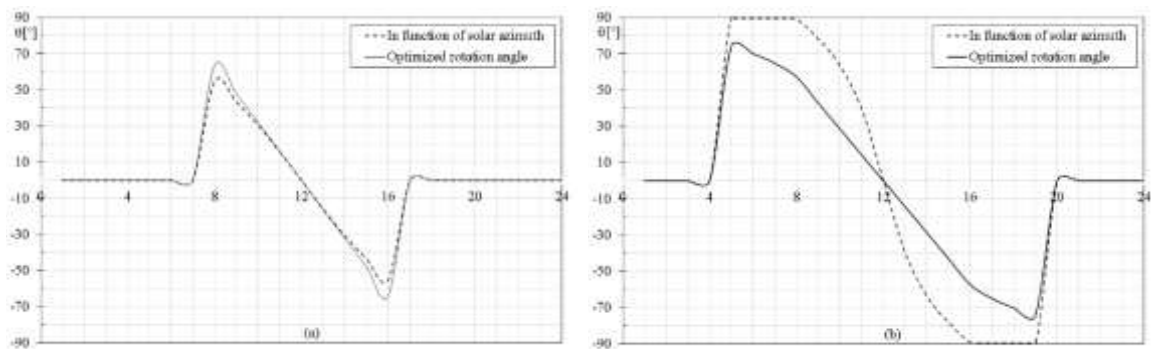


Fig. 2: Trend of the rotation panel angle in function of the optimized angle and in function of the solar azimuth angle for a winter day (a) and a summer day (b)

In winter, the deviations are negligible; only during the first and the last hours of the day are the differences evident and equal about to  $10^\circ$ . In summer the deviations are more marked, by observing an optimized rotation angle always lower than the solar azimuth value; these differences can be also greater than  $30^\circ$  during the mid-morning and the mid-afternoon.

### 3. Self-shading analysis

The distance between two consecutive modules must be adequately chosen in order to avoid shading effects during panel rotation. These phenomena are marked in the first and in the last hours of the day, therefore a parametric analysis was conducted. To avoid total shading effects, the relation between the module spacing  $D$ , the module width  $W$  and the solar path is shown in Fig. 3, with reference to the y-z plane of Fig. 1.

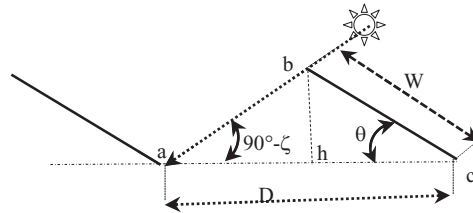


Fig. 3 – Evaluation of the shaded surface in two consecutive strings

The triangles  $abh$  and  $bch$  are similar, therefore:

$$(W^2 + D^2 - 2 \cdot W \cdot D \cdot \cos[\theta])^{\frac{1}{2}} \cdot \cos[\zeta] = W \cdot \sin[\theta] \quad (7)$$

that relates the rotation angle  $\theta$  and the zenith angle  $\zeta$ . In Fig. 4.a the trend of a critical zenith angle  $\zeta^*$  beyond which a shading effect on the module surface is produced, for different values of the ratio  $D/W$ , and in function of the rotation angle  $\theta$ , is reported.

For a module rotation of  $40^\circ$ , the deviations between the critical angles  $\zeta^*$  are more marked, ranging from  $22.1^\circ$  to  $71.6^\circ$  respectively for  $D/W=1$  and  $D/W=2.7$ , but the shading effects result already more limited for a ratio  $D/W=1.5$  and for rotation angles greater than  $30^\circ$ . If  $\theta$  is lower than  $30^\circ$ , the shading effect is produced only for zenith angles higher than  $60^\circ$ , a situation which occurs mainly in the first and in the last hours of the day. In Tab. 2, by a simulation carried out with the TRNSYS code, the collected beam solar radiation in function of the ratio  $D/W$  by setting  $\beta_a=30^\circ$  for both the considered rotation strategies is reported. Fig. 4.b shows the shaded fraction  $F$  for three different  $D/W$  values with optimized rotation.

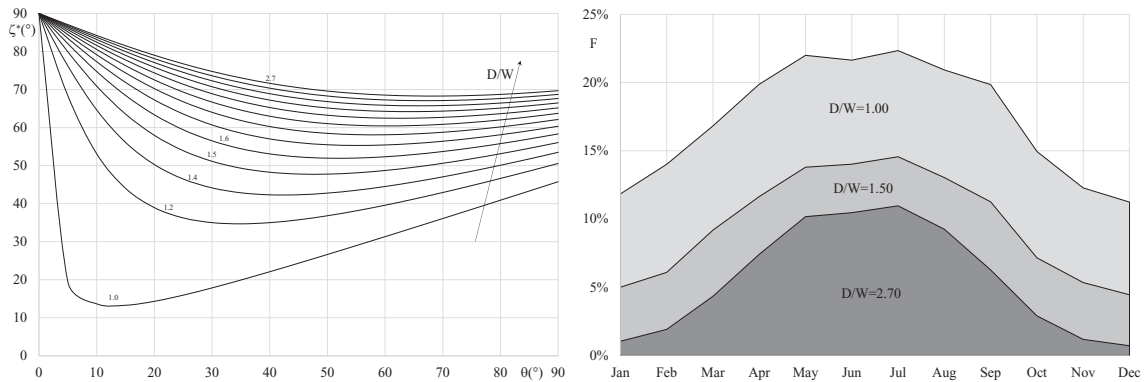


Fig. 4 – (a) Relation between rotation and solar zenith angles in function of different ratio  $D/W$ ; (b) – Cosenza: beam radiation shading factor for three different values of the ratio  $D/W$

The increment of the ratio  $D/W$  from 1.00 to 1.50 produces a collected beam radiation growth of 9.6%. Passing from 1.50 to 2.70, a more limited increment of 4.5% was observed. The simpler control strategy always produce worse results of about 35% compared to the ideal value of 1998 kWh/m<sup>2</sup> per year, determined in absence of shading effects. The beam radiation shading factor decreases strongly passing from  $D/W=1.00$  to  $D/W=1.50$ , while for greater values the same factor decreases slightly.

Table 2 – Cosenza: beam solar radiation collected on the modules in kWh/m<sup>2</sup> in function of the ratio  $D/W$  by considering shading effects

	$\theta$ =Solar azimuth D/W			$\theta$ =optimized rotation angle D/W		
	1.00	1.00	1.50	2.70	1.50	2.70
Jan	67	72	78	81	74	79
Feb	87	95	104	108	95	101
Mar	118	140	153	161	130	134
Apr	108	146	161	168	119	116
May	108	167	184	192	117	105
Jun	114	193	212	221	123	106
Jul	120	197	217	226	131	114
Aug	133	190	208	218	145	137
Sep	122	149	165	174	133	133
Oct	92	104	113	118	101	107
Nov	80	87	94	98	88	95
Dec	78	83	90	93	85	91
Yearly	1229	1623	1779	1860	1340	1319

## 1. Conclusions

The beam solar radiation collected on particular types of PV modules, which must be very light in order to make the tracking system less energy intensive, has been quantified by supposing the adoption of two different control strategies. The first simple one rotates the module of an angle equal to the solar azimuth angle, and adjusts it during the summer sunrise and sunset. In the second control strategy, the rotation angle is chosen in order to minimize the incident angle during the whole year. By considering a horizontal tracking axis system oriented toward south and tilted of 30°, the first control strategy, compared to a fixed system with the same inclination, allows a collected beam radiation growth of 23.6% at annual level. A correspondent tracking efficiency of 91.4%, evaluated in function of the direct normal incident radiation, has been determined. The second control strategy allows a collected beam radiation growth of the 27.5% at annual level, and the correspondent tracking efficiency is 96.4%. A parametric study in function of the ratio between the tracking axis spacing ( $D$ ) and the module width ( $W$ ) has been carried out to evaluate the self-shading effects. The employment of a  $D/W$  ratio greater than 1.50 leads to negligible improvements, while passing from  $D/W=1.00$  to  $D/W=1.50$ , an increment of the 9.1% and of the 9.6% of the collected beam radiation respectively for the first and the second control strategy was observed. For the considered locality, a fixed PV system tilted of 30° allows the obtainment of 1431 kWh/kWp. The investigated single axis tracker with the same axis inclination and an optimized rotation angle, allows for the achievement of 1734 kWh/kWp (+21%) with a ratio of  $D/W=1$ , 1901 kWh/kWp (+32.8%) with a ratio  $D/W=1.50$  and 1987 kWh/kWp (+38.8%) for  $D/W=2.70$ . Therefore, in the analysed PV system, for an equal available surface, the increment of the collected beam radiation always prevails over the reduction of the installable PV peak power.

## References

- [1] Mousazadeh H., Keyhani A., Javadi A., Mobli H., Abrinia K., Sharifi A., *A review of principle and sun-tracking methods for maximizing solar systems output*. Renewable and Sustainable Energy Reviews 13 (2009) 1800–1818
- [2] Pavel Y.V., Gonzalez H.J., Vorobiev Y.V., *Optimization of the solar energy collection in tracking and non-tracking PV solar system*. In: Proceedings of the 1st international conference on electrical and electronics engineering, ICEEE; 2004. p. 310–314
- [3] Helwa N.H., Bahgat A.B.G., Shafee A.M.R.E., Shenawy E.T.E., *Maximum collectable solar energy by different solar racking systems*. Energy Sources 2000;22:23–4.
- [4] Chicco G, Schlabbach J, Spertino F., *Performance of grid-connected photovoltaic systems in fixed and sun-tracking configurations*, 2007. <http://www.labplan.ufsc.br/congressos/PowerTech07/>.
- [5] Abu-Khader M. M., Badran O. O., Abdallah S., *Evaluating multi-axes sun-tracking system at different modes of operation in Jordan*. Renewable and Sustainable Energy Reviews 12 (2008) 864–873.
- [6] Al-Mohamad A., *Efficiency improvements of photo-voltaic panels using a Sun-tracking system*. Applied Energy 79 (2004) 345–354.
- [7] Huang B.J., Ding W.L., Huang Y.C., *Long-term field test of solar PV power generation using one-axis 3-position sun tracker*. Solar Energy 85 (2011) 1935–1944.
- [8] Huang, B.J., Sun, F.S., 2007. *Feasibility study of 1-axis three-position tracking solar PV with low concentration ratio reflector*. Energy Conversion and Management 48, 1273–1280.
- [9] Koussa M., Cheknane A., Hadji S., Haddadi M., Noureddine S., *Measured and modelled improvement in solar energy yield from flat plate photovoltaic systems utilizing different tracking systems and under a range of environmental conditions*. Applied Energy 88 (2011) 1756–1771.
- [10] Jinayim T., Arunrungrasmi S., Tanitteerapan T., Mungkung N., *Highly efficient low power consumption tracking solar cells for white LED-based lighting system*. International Journal of Electrical Computer and Systems Engineering 2007;1(2):1307–5179.
- [11] VV.AA., *TRNSYS 17, A transient simulation program*, Solar Energy Laboratory, University of Wisconsin, Madison (USA)
- [12] Duffie J.A., Beckman W.A., *Solar Engineering of Thermal Processes*, 4th Edition, Ed. Wiley, Hoboken, NJ (USA)
- [13] Marion W.F., Dorian A.P., *Rotation Angle for the Optimum Tracking of One-Axis Trackers*, Technical Report NREL, 2013